

SUPPORTING INFORMATION FOR THE ARTICLE

**Urease Catalyzed High-Density Sodium Alginate
Microspheres Enables High Oral Bioavailability of
Macromolecular Drugs**

**Yicheng Jiang ^a, Li Mi ^a, Xiang Xu ^{a, c}, Adric Hii Ru Khiing ^a, Zhenghong Wu ^{a, *},
and Xiaole Qi ^{a, b, *}**

*^a Key Laboratory of Modern Chinese Medicines, China Pharmaceutical University,
Nanjing 210009, PR China.*

*^b Industrial Technology Innovation Platform, Zhejiang Center for Safety Study of Drug
Substances, Hangzhou 310018, China.*

*^c King's College London, Institution of Pharmaceutical Science, Franklin Wilkins
Building, 150 Stamford St, London SE1 9NH, England.*

*Corresponding author. Tel./fax: +86 15062208341 (Zhenghong Wu); +86 25
83179703 (Xiaole Qi).

E-mail address: zhenghongwu66@cpu.edu.cn (Zhenghong Wu),
qixiaole523@cpu.edu.cn (Xiaole Qi)

Synthesis of FITC labeled sodium alginate

The synthesis method of FITC labeled was referred to the previous reported method¹. First, 360 mg of SA, 150 mg of 1-(3-Dimethylaminopropyl)-3-ethylcarbodiimide hydrochloride (EDC), and 90 mg of N-Hydroxy succinimide (NHS) were accurately weighed and added into 60 mL of pH 5.0 sodium acetate buffer. EDC/NHS in this system was used to activate the carboxyl in SA. The mixture was stirred to ensure SA was fully dissolved. After that, adding 201 μ L of ethylenediamine to the mixture and continued stirring for 4 h. 20 mL of isopropanol was dropwise added to the system under stirring until no more precipitate formed. The mixture was then centrifuged at 10000 rpm for 10 min. After the supernatant was removed, the solid at the bottom and 1 mg of Fluorescein isothiocyanate isomer (FITC) was added to 48 mL of pH 8.5 sodium bicarbonate solution to react for 4 h. After the reaction, 20 mL of acetone was added to precipitate FITC-labeled SA. At last, using methanol to wash the sediment to remove the unbound FITC. The remaining residue was dispersed with appropriate water and then freeze-dried to obtain FITC-labeled SA powder.

Mucin purification

Healthy rabbits (female, 2.0~2.2 kg) were fasted for 8 hours and sacrificed. Their stomachs were quickly excised and cut open along the luminal line. The interior gastric surface was washed thrice with 37 °C normal saline to remove the food residues, and the mucus layer was collected via scraper. The obtained mucus was stirred in icy PBS containing 5 mM EDTA for 4 h to remove all the metal ions. The mixture was then centrifuged, and the purified mucus was kept in 4 °C PBS.

Establishing diabetes rat model

The diabetic rat model was established by the method reported with slight modifications². SD rats (male, 6-8 w) were fed with a high-sugar and high-fat diet, which consisted of 10% sucrose, 10% lard, and 5% cholesterol for 1 month to induce insulin resistance. Further injecting intraperitoneally streptozocin (STZ) with a 55 mg/kg dose for consecutive 7 days to cause diabetes. After 7 days, the fasting blood glucose of rats was measured by a glucometer. Finally, rats with blood glucose levels greater than 13.5 mmol/L were chosen for the formal experiment and fed a high-sugar and high-fat diet for another 3 weeks.

Establishing diabetes mouse model

The diabetes mouse model was established via the previously reported method with slight modifications^{3, 4}. Mice (female, 6-8 w) were fed a normal diet for a week, and their blood glucose levels were measured simultaneously every day by using the glucometer (Sinocare, China). One week later, streptozocin (STZ) was injected intraperitoneally with a dose of 120 mg/kg to induce the acute injury of islet β cells, and mice were fed with a normal diet for another week. The final step is measuring the fasting blood glucose and choosing the mice whose BGL is higher than 11.5 mmol/L as the successful acute diabetes mouse model.

Biosafety assessment

4 groups of type II diabetes rats were pre-treated with the same dose of normal saline (NS), insulin (Ins), Ins@SA microspheres, and the Ins/Ur/MgO@SA microspheres by

gavage. After 8 h, 1 mL of orbital venous blood was collected from rats for blood routine tests. Then, the rats were sacrificed, their stomach and upper intestine were dissected, cleaned, and soaked with formalin. H&E staining analysis of the samples was performed to observe whether pathological changes occurred (Berke Bio Tech Inc., Nanjing).

The biosafety assessment of the Ins/Ur/MgO@SA microspheres in the diabetes mice model is similar to that in the type II diabetes rat model. After the pre-treatment of four formulations, the stomach, intestine, and 1 mL of orbital venous blood of mice were collected and sent to the Berke Bio Tech Inc. for H&E staining analysis and blood routine test.

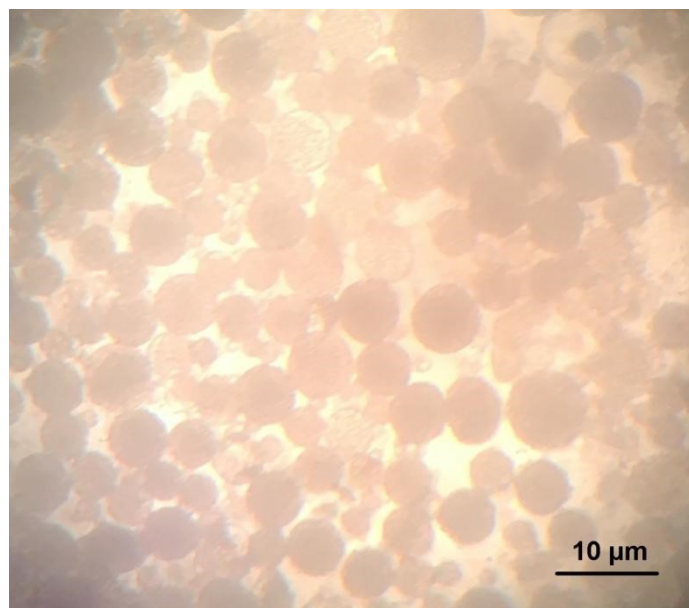


Fig. S1. The optical microscope images of the SA microspheres prepared by the emulsification method.

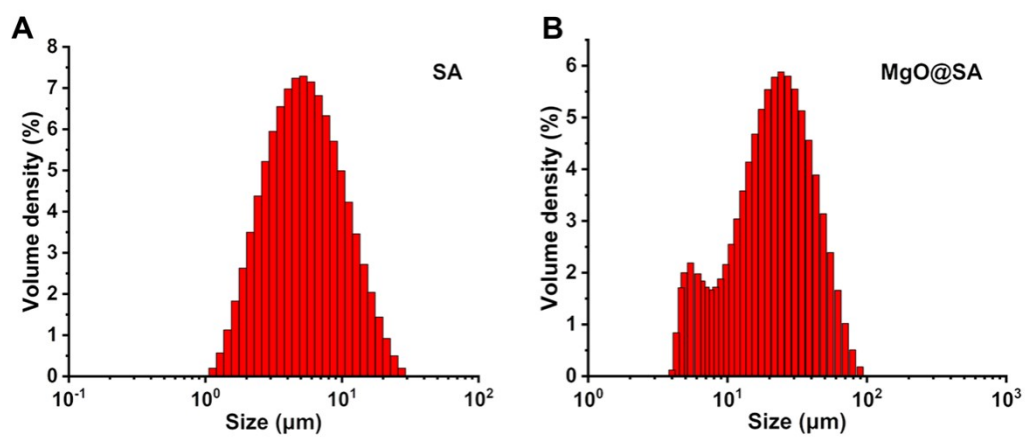


Fig. S2. Size distribution (d , μm) results of A) the SA and B) the MgO@SA microspheres.

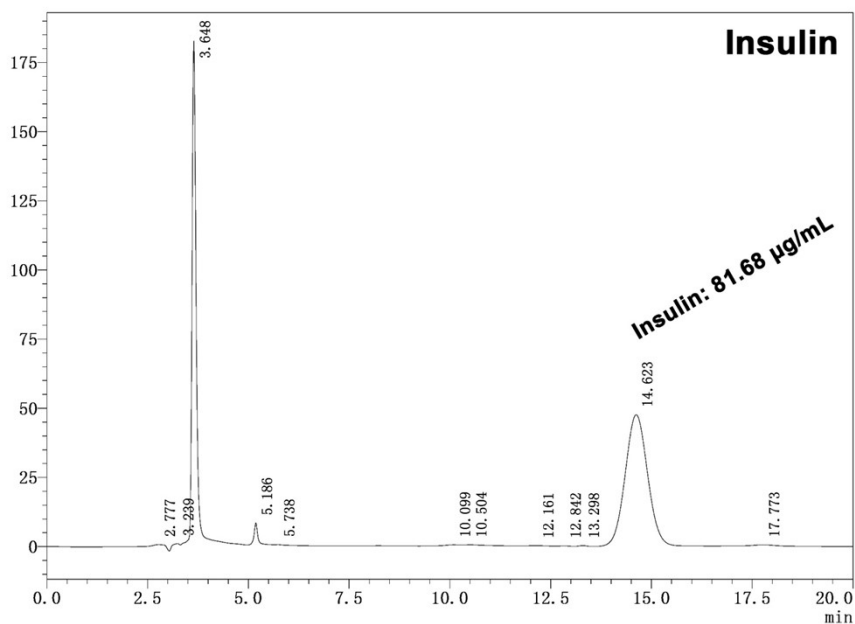


Fig. S3. The FTIR spectrum of the insulin solution (detection wavelength: 214 nm).

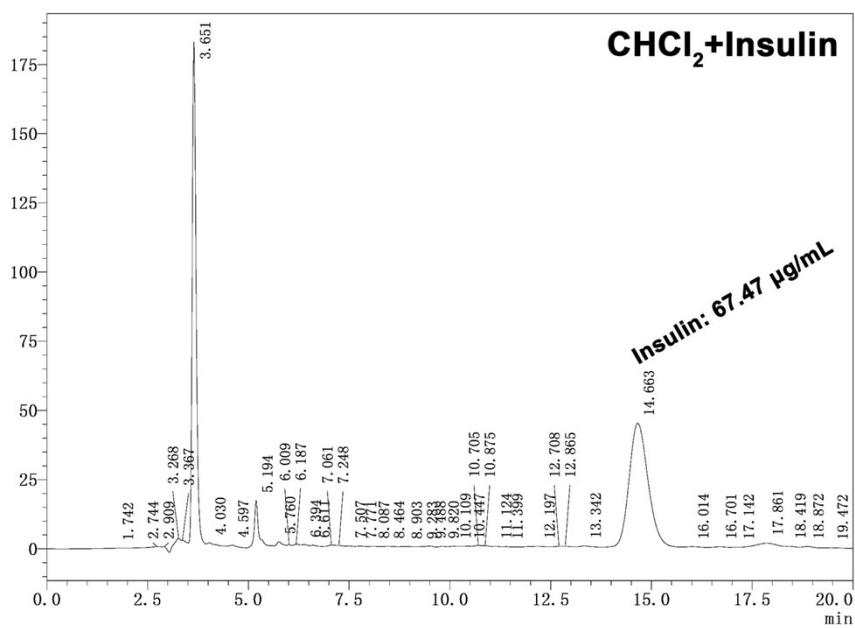


Fig. S4. The FTIR spectrum of the insulin solution after incubated with dichloromethane (detection wavelength: 214 nm).

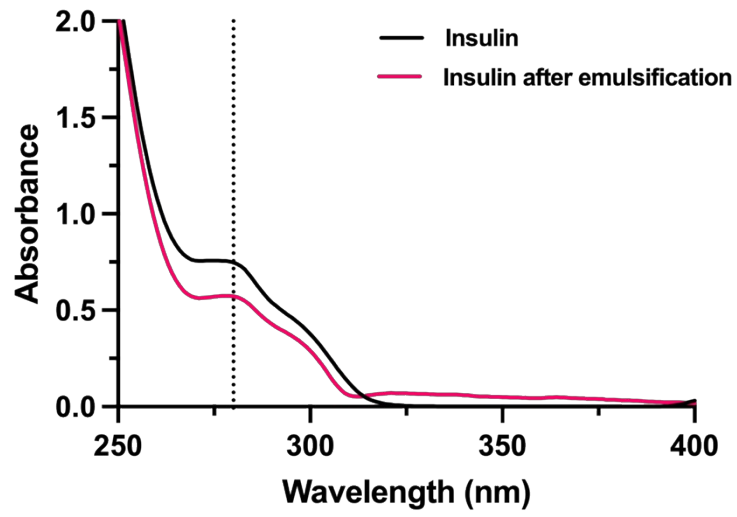


Fig. S5. The UV-Vis spectra of the insulin and the insulin after emulsification.

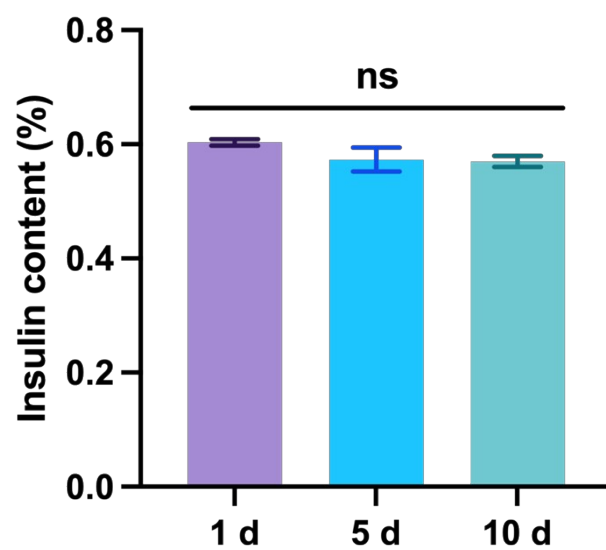


Fig. S6. The insulin content of the Ins/Ur/MgO@SA microspheres in 1, 5, and 10 days at room temperature in dark (n=3). (ns represent there is no significant difference among these groups.)

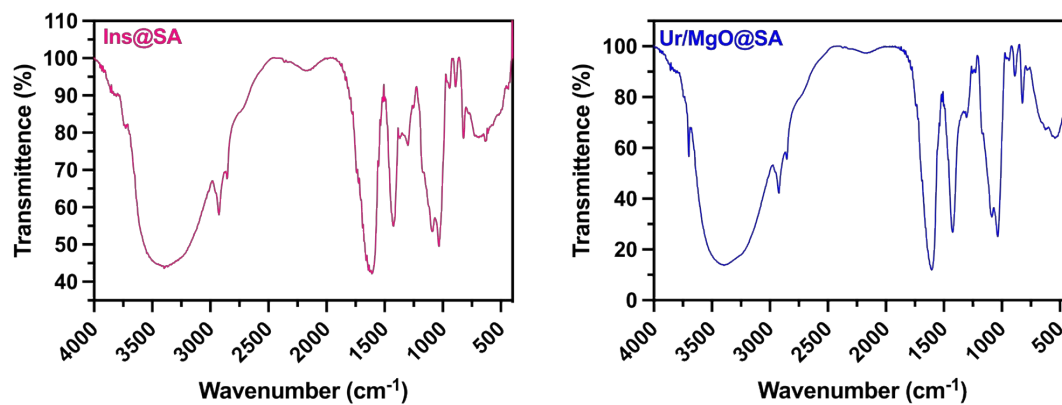


Fig. S7. FTIR spectra of A) the Ins@SA microspheres and B) the Ur/MgO@SA microspheres

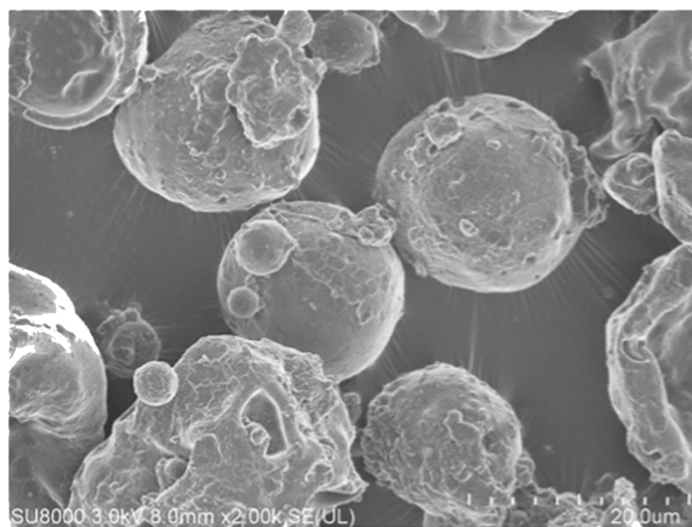


Fig. S8. The SEM images of the Ins/Ur/MgO@SA microspheres.

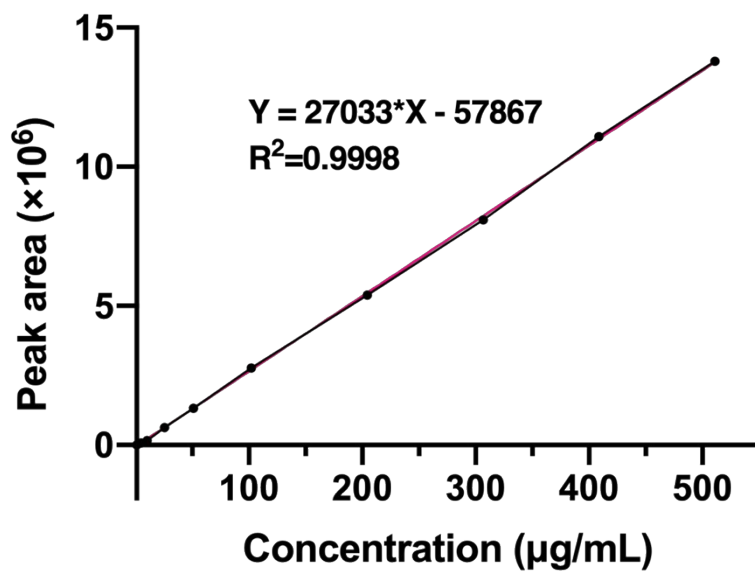


Fig. S9. The standard curve for HPLC analysis of insulin (214 nm).

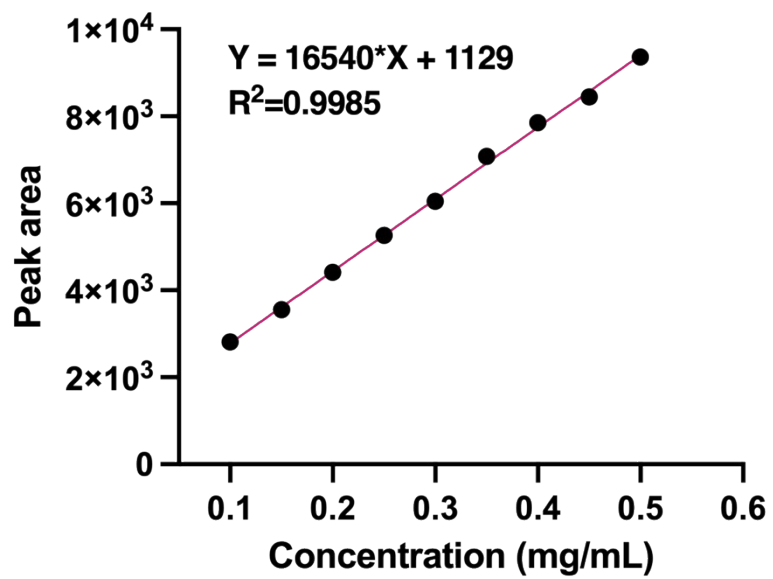


Fig. S10. The standard curve for HPLC analysis of urea (190 nm).

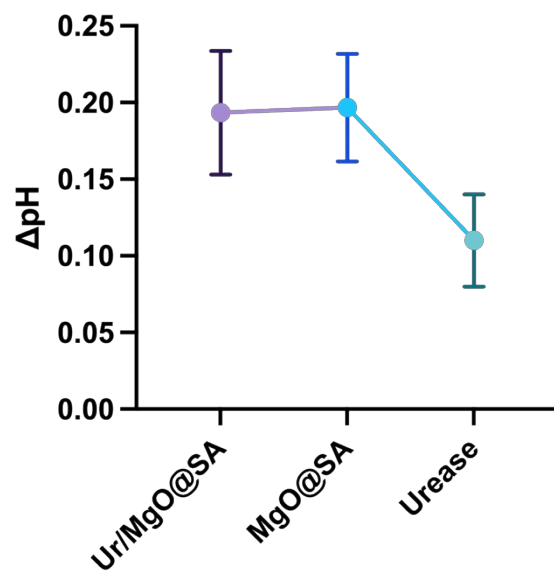


Fig. S11. The pH change value of solution in the Ur/MgO@SA, MgO@SA, and urease groups after incubated with urea (n=3).

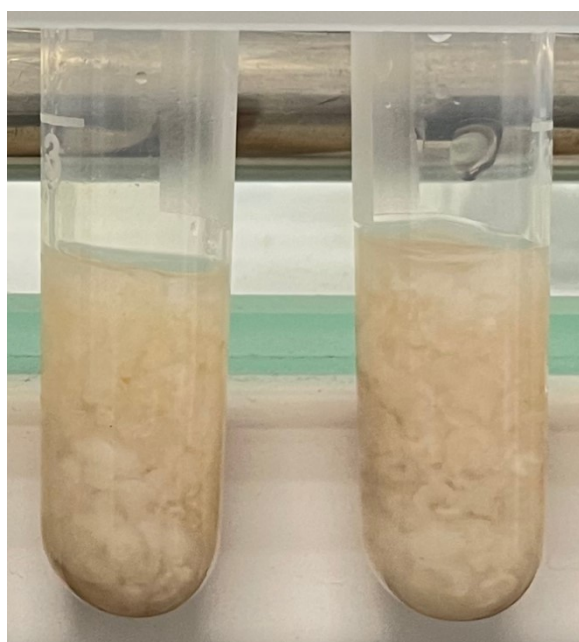


Fig. S12. The fresh rabbit gastric mucus after purification.

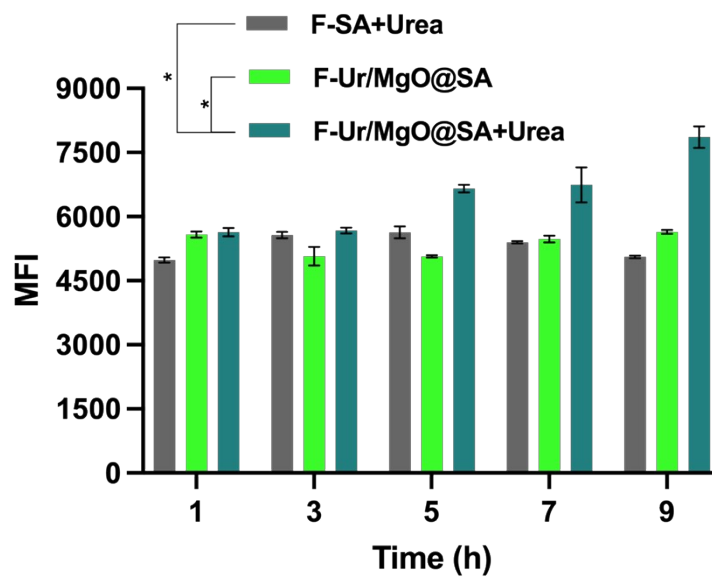


Fig. S13. The semi-quantitative analysis chart of mean fluorescence intensity (MFI) in different groups (n=3, *p < 0.05).

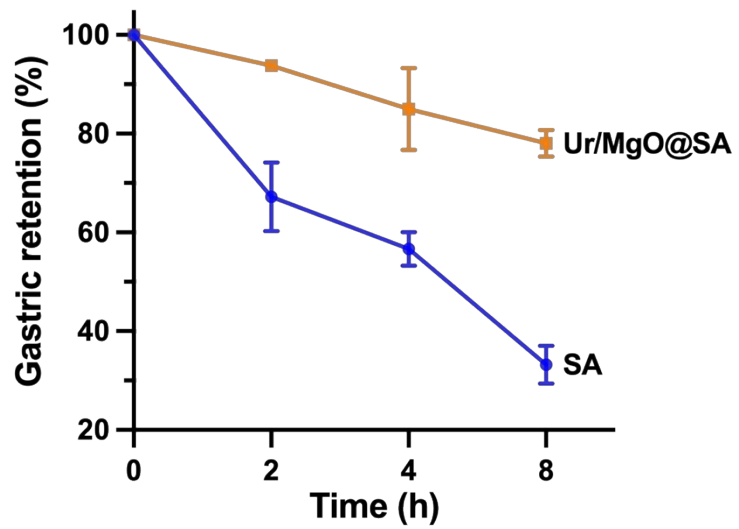


Fig. S14. Gastric retention percentage curve of two groups. Gastric retention was calculated as the ratio between the initial (0 h) intensity and the intensity at the following time points (n=3).

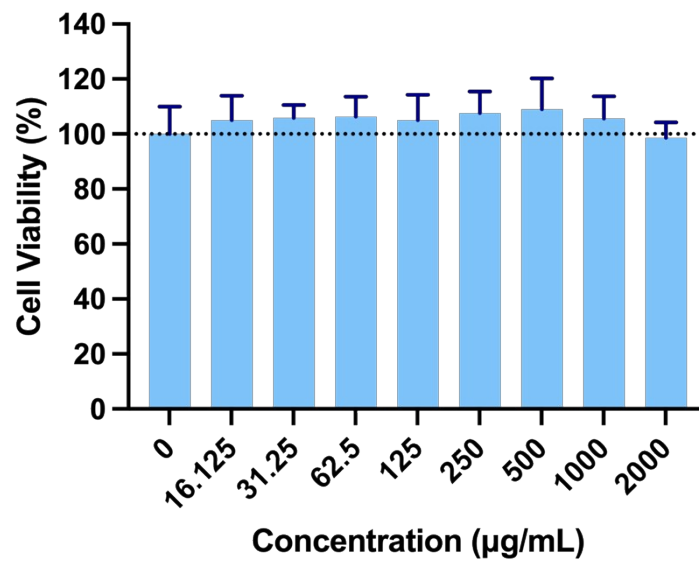


Fig. S15. The cell viability of Caco-2 cells incubated with different concentrations of the Ins/Ur/MgO@SA microspheres (n=6).

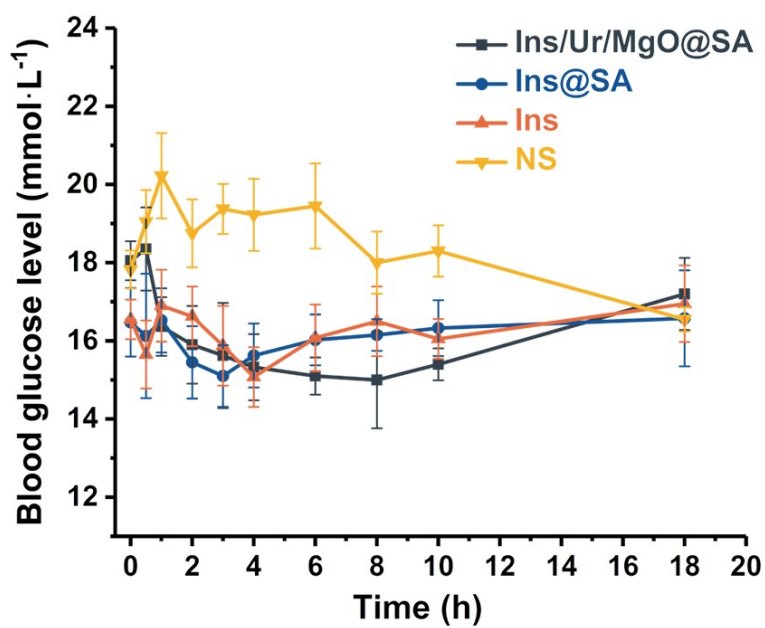


Fig. S16. A) Blood glucose level ($\text{mmol}\cdot\text{L}^{-1}$) variation of rats after treated with the Ins/Ur/MgO@SA microspheres, the Ins@SA microspheres, insulin (Ins), and saline (NS) respectively ($n=4$).

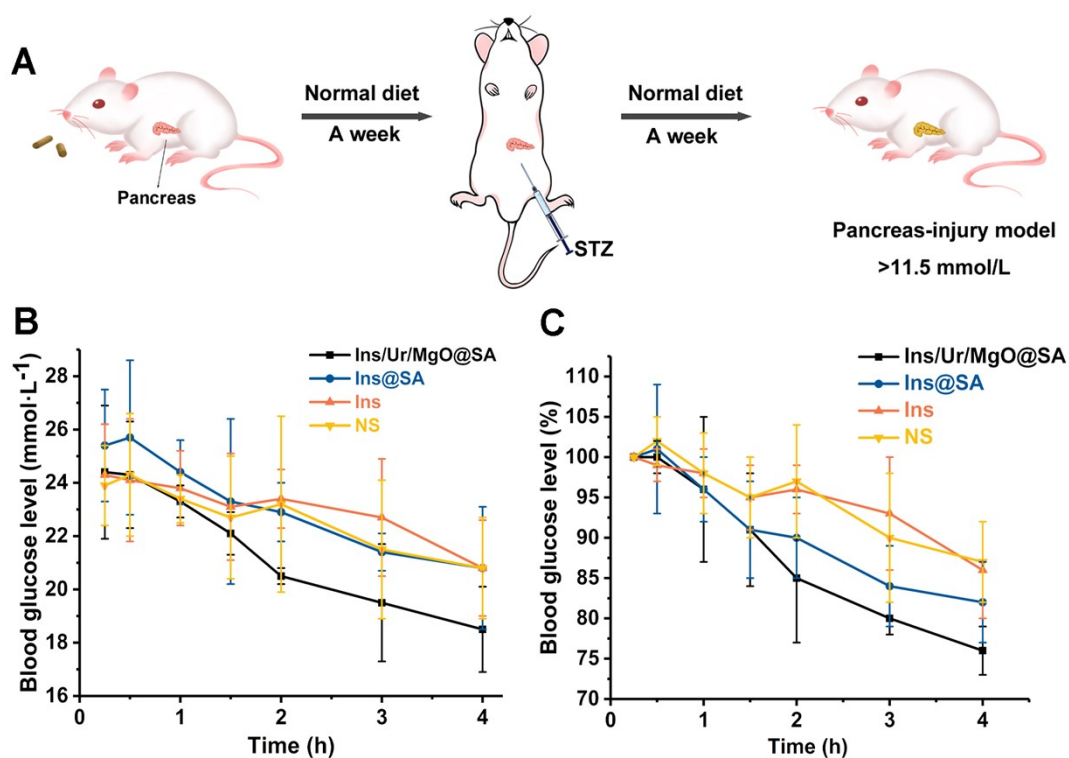


Fig. S17. A) The establishing of diabetes mice model; B) blood glucose level ($\text{mmol}\cdot\text{L}^{-1}$) variation of mice after treated with the Ins/Ur/MgO@SA microspheres, the Ins@SA microspheres, insulin (Ins), and saline (NS) respectively ($n = 5$); C) blood glucose level (percentage) variation of mice after treatment with the Ins/Ur/MgO@SA microspheres, the Ins@SA microspheres, insulin (Ins), and saline (NS) respectively ($n=5$).

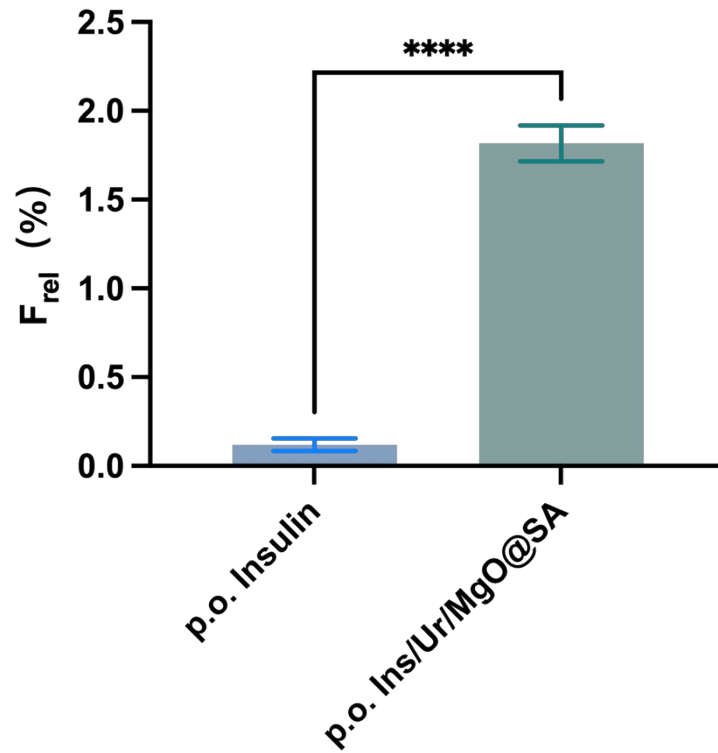


Fig. S18. Relative oral bioavailability of insulin in different groups ($n = 4$, **** $p < 0.0001$ represent significant differences compared to the *p.o.* Ins/Ur/MgO@SA group).

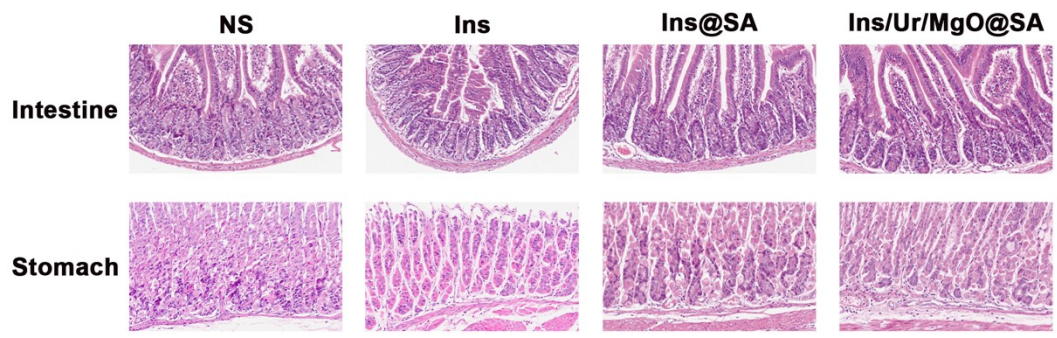


Fig. S19. H&E staining images of stomach and intestine of mice 7 days after intragastric administration of saline, insulin, Ins@SA microspheres, and Ins/Ur/MgO@SA microspheres, $\times 200$.

Table S1. Particle size distribution of the SA, MgO@SA, and the Ur/MgO@SA microspheres.

	D50 (μm)	D90 (μm)	Uniformity	Span
SA	5.57	18.3	0.605	1.961
MgO@SA	22.1	36.9	1.592	6.001
Ins/Ur/MgO@SA	12.2	13.3	0.949	2.882

Table S2. Density results of the SA, MgO@SA, and the Ur/MgO@SA microspheres (n=3).

□	Bulk Density (g/cm ³)	RSD	Tap Density (g/cm ³)	RSD	Apparent Density (g/cm ³)	RSD
SA	0.318	0.017	0.550	0.005	0.645	0.016
MgO@SA	0.344	0.004	0.569	0.046	1.552***	0.021
Ur/MgO@SA	0.353	0.034	0.568	0.048	1.498***	0.006

*** $p < 0.001$ represent significant differences compared to the SA group.

References

1. Ning, X.; Yao, C.; Guan, L.; Bai, Y., Fluorescent Sodium Alginate Applied to Papermaking Furnish with Polyamideamine Epichlorohydrin. *Bioresources* **2018**, *13* (4), 7519-7533.
2. Luo, Z.; Fu, C.; Li, T.; Gao, Q.; Miao, D.; Xu, J.; Zhao, Y., Hypoglycemic Effects of Licochalcone A on the Streptozotocin-Induced Diabetic Mice and Its Mechanism Study. *Journal of Agricultural and Food Chemistry* **2021**, *69* (8), 2444-2456.
3. Fukuda, K.; Tesch, G. H.; Yap, F. Y.; Forbes, J. M.; Flavell, R. A.; Davis, R. J.; Nikolic-Paterson, D. J., MKK3 signalling plays an essential role in leukocyte-mediated pancreatic injury in the multiple low-dose streptozotocin model. *Laboratory Investigation* **2008**, *88* (4), 398-407.
4. Lechner, A.; Yang, Y. G.; Blacken, R. A.; Wang, L.; Nolan, A. L.; Habener, J. F., No evidence for significant transdifferentiation of bone marrow into pancreatic β -cells in vivo. *Diabetes* **2004**, *53* (3), 616-623.